Penerbit Akademia Baru

Journal of Advanced Research in Fluid Mechanics and Thermal Sciences

Journal homepage: www.akademiabaru.com/arfmts.html
ISSN: 2289-7879

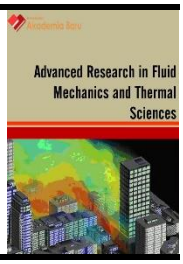

Torque Characterization of T-shaped Magnetorheological Brake Featuring Serpentine Magnetic Flux

Open Access

Ilham Rizkia Nya'Ubit[1], Gigih Priyandoko[2], Fitrian Imaduddin[1], Dimas Adiputra[3], Ubaidillah[1,*]

[1] Mechanical Engineering Department, Universitas Sebelas Maret, Jalan Ir. Sutami 36A, Kentingan, Surakarta 57126, Indonesia
[2] Electric Engineering Department, Universitas Widya Gama, Malang, Jawa Timur, Indonesia
[3] Institut Teknologi Telkom (IT Telkom), Surabaya, East Java, Indonesia

ARTICLE INFO

Article history:
Received 27 August 2020
Received in revised form 1 October 2020
Accepted 1 October 2020
Available online 9 December 2020

ABSTRACT

Recently, T-shaped Magnetorheological Brake (MRB) usually utilize more than one wire coil electromagnetic to maximize magnetic flux reaching all Magnetorheological Fluid (MRF) gaps. This research was focused on the usage of a single wire coil on MRB with uniformly magnetic flux distribution. To achieve the goal, the serpentine magnetic flux profile was adopted to maximize all MRF gaps that only use a single coil. Firstly, the magnetic circuit which implementing serpentine magnetic flux was design in a two-dimensional model. It was then followed by magnetostatic simulation using Finite Element Method Magnetics (FEMM) to determine the amount of magnetic flux density. The data were then employed to calculate the braking torque. After having the final dimension and completing the workshop drawing, an MRB prototype was fabricated. Thus, the prototype was characterized using the braking test apparatus to figure out the torque profiles. Moreover, the experimental results were compared to the simulation results. This process justified the validity of the proposed mathematical model of the T-shaped MRB. It was investigated that the maximum braking torque from simulations and experimental works were 1.51 Nm and 1.91 Nm at 1 A, respectively. Overall the between differences of simulations and experimental works were about 10%. It is therefore, the mathematical model can be used for further application in the actuator control system.

Keywords:
Magnetorheological fluid; magnetorheological brake; torque sensor

1. Introduction

Magnetorheologicals are part of smart materials because their properties can be changed by the magnetic field [1]. There are many types in magnetorhelogicals, that are magnetorheological fluid (MRF) that liquid phase [1], magnetorheological elastomer that composite of elastomer and magnetic

* *Corresponding author.*
E-mail address: ubaidillah_ft@staff.uns.ac.id

https://doi.org/10.37934/arfmts.78.2.8597

particle-like Waste Tire Rubber (WTR) [2] and natural rubber [3], and magnetorheological foam that magnetorheological elastomer with the porous microstructure [1].

MRF is the mixture of micron size magnetizable iron particles with non-magnetic carrier fluid [4–8]. Typically, it contains ferromagnetic particles [4] and a synthetic or silicone-based oil [9]. It is a very responsive material that could react in milliseconds subjected to a magnetic field [5,8,10,11]. The properties change in conjunction with the increment of viscosity because the magnetic field particles start to make a line along the flux path, so that makes a bond like-chain [5,6,8,12].

In every device of MRF, there are three basic operations, that are direct shear type, valve type, and squeeze type [4,6,10,13]. All of them are identic with MRF, which is located between two magnetic surfaces. Direct shear type identic with two plates that one of them rotate and another one is fixed. Valve type identic with two plates set with MRF flowing pass through them. Squeeze type identic with two plates pushed MRF to come out.

For two decades, there were many types of research about MRF because of its responsiveness, low power, and tidy structure subjected to the magnetic field [1,7,14]. An example of daily needs that could be used from MRF was for automotive industries and health that were developed in the form of magnetorheological brakes (MRB) [12,15–18].

MRB is a device in the mechanical field that controls brake torque using the magnetorheological principle[6]. It has advantages over conventional hydraulic brake (CHB) system [15,19,20]. It's basic designs are disc, drum, and hybrid [5,10,15]. Those designs utilize an effective area from the MRF gap to improve the performance. Disc utilizes the annular gap, drum utilizes the radial gap, and hybrid uses both annular and radial gaps.

There were many ways to enhance the torque performance of MRB such as meandering flow in the core of MRB, adding the number of turn wire and the number of the disc, making a T-shaped rotor to get more MRF gap, and combining magnetic and non-magnetic material on stator or rotor which is called serpentine magnetic flux [11,17,21–27]. Serpentine magnetic flux has an advantage in increasing torque more effectively because it can manage the magnetic flux path by deflecting it.

Some T-shaped MRB was proposed earlier. It was found that they took more than one coil to reach a good and effective magnetization area that could get all MRF gaps. For example, Nguyen [26] and Avraam [17] had made MRB T-shaped with two coils. However, it would be consuming more power due to the needs of multi-coil. Ubaidillah predicted MRB serpentine type that could maximize magnetic flux only uses a single coil [27]. Hidayatullah also made the prediction torque with the combination of T-shaped type and serpentine flux to get more MRF gap with small size[25]. However, this MRB can be made more effective.

The T-shaped MRB was proposed using a single-coil and featuring serpentine magnetic flux flow similar to Hidayatullah with a smaller design and different materials. The simulation was presented and then fabricated the prototype to characterized the real-time torque using the braking test apparatus. Both simulation and experimental work were compared to get the validation for future research.

2. Methodology

2.1 Design of T-Shaped Magnetorheological Brake

Figure 1 shows the design of MRB. Its casing contains a stator and a cover that has a screw at the end of it. Screw and nut on casing had the advantage to overhaul part of the MRB easily. The screw was made on the shaft and rotor to ensure the shaft remains connected to the rotor. AWG 28 copper wire was used to generate a magnetic field. The combination of magnetic and non-magnetic materials on the stator has the function to control the magnetic flux path that can turn the flux path

reaching the outer annular gap. Magnetic material on the casing and rotor let flux across the MRF gap. Non-magnetic material on the bobbin is used to ensure the flux not reaching the coil. MRF gap was between the rotor and stator. Seals and bearings were added to prevent the leakage and translational motion on the shaft. Table 1 shows detailed information about parts of MRB.

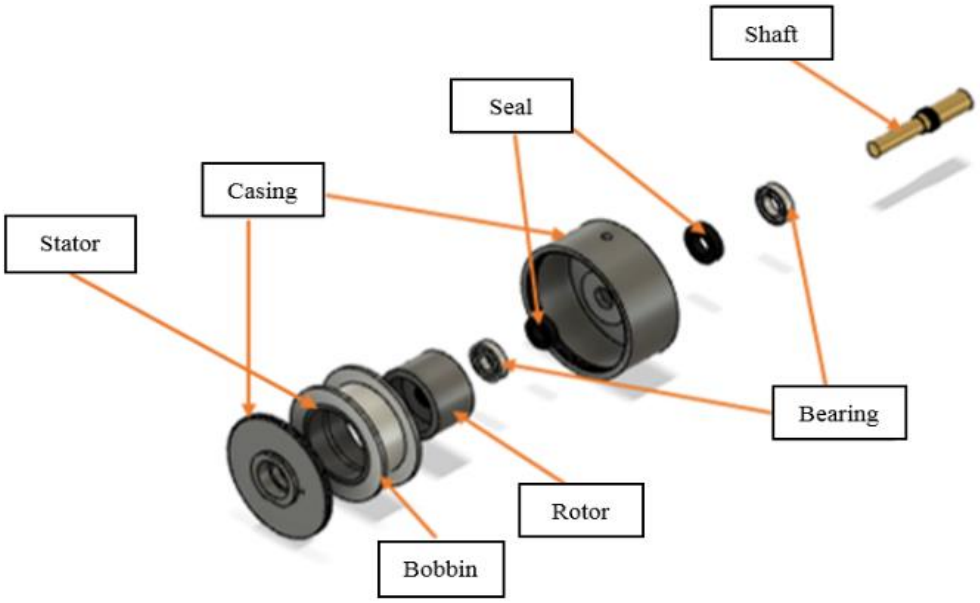

Fig. 1. Design of MRB T-shaped serpentine flux

Table 1
Part list of MRB

Part	Type	Material
Casing	Magnetic	S45C Steel
Stator Magnetic	Magnetic	S45C Steel
Stator Non-Magnetic	Non-Magnetic	Aluminium
Bobbin	Non-Magnetic	Aluminium
Shaft	Non-Magnetic	Copper
Rotor	Magnetic	S45C Steel
Coil	Non-Magnetic	Copper Wire
Seal	Non-Magnetic	Standard
Bearing	Magnetic	Standard

MRF-132DG LORD Corp [28] was used that suitable for shear and valve type application. It has micron size particles, and the color is leaning like iron. The location is between the casing, stator, and rotor called the MRF gap. In non-magnetic field conditions, it had low viscosity so that MRB could rotate in small force. Table 2 shows the properties of MRF-132DG.

Table 2
Properties of MRF-132DG

Property	Value
Appearance	Dark grey liquid
Viscosity, Pa-s	0.112
Density, g/cm^3	2.95-3.15
Solid content by weight, %	80.98
Flashpoint, ^{o}C	>150
Operating Temp., ^{o}C	-40 to +130

2.2 Magnetostatics Simulation

Magnetic field analysis is necessary to find how effective magnetic flux generated. It is also necessary to determine magnetic flux density which used for braking torque. Reluctance for each part can be known from Eq. (1) [19,25,27]

$$R = \frac{L}{\mu A} \tag{1}$$

where L is the distance passed by the magnetic flux in each section, μ is magnetic permeability, and A is an effective area from the magnetic flux path. Based on the circuit, Eq. (2) describes the total of reluctance

$$\Sigma R = R_{coil} + R_{wall} + R_{MRF} + R_{rotor} + R_{MRF} + R_{stator\ steel} + R_{MRF} + R_{rotor} + R_{MRF} + R_{stator\ steel} + R_{MRF} \tag{2}$$

The electromotive force can be expressed in Eq. (3) [25]

$$\Sigma F = \phi \Sigma R = NI \tag{3}$$

where ϕ, N, and I respectively are magnetic flux, wire turn, and current passed the wire turn.

However, the result would give a big error using those equations are because they are used to simplify the work. It should have a significant error in the experimental situation. It needs a complicated method that shows in every part of MRB. Therefore, the finite element method is used to fix the solution.

Finite Element Method Magnetics (FEMM) 4.2 was used for magnetic simulation [29]. FEMM is a simulation software that has the function to identify, solve, and show the result 2D problem in planar or asymmetric from magnetostatics, eddy current, and electrostatic through finite element method. There are a lot of materials that can be used in the FEMM library. It could also add the new material and custom it as needed. It will display the distribution of density flux magnetic in every part of the material that cannot do in the experiment result. Figure 2 and Table 3 show the design and condition of FEMM in the asymmetric model.

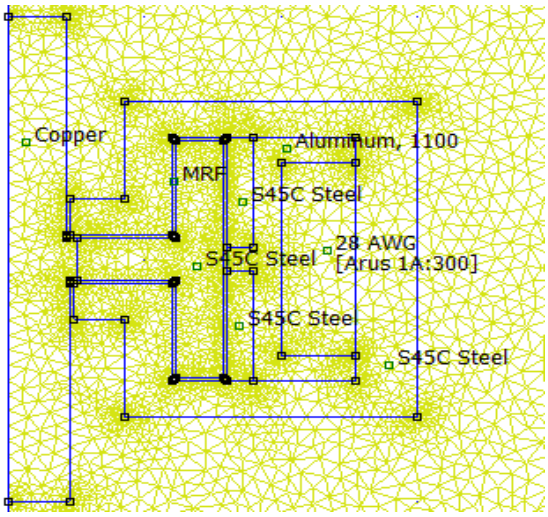

Fig. 2. Design of Simulation FEMM

Table 3
Condition of simulation FEMM

Symbol	Value
Mesh	9190
Element	18051
Problem Type	Axisymetry
Length	mm
Boundary Condition	Air

2.3 Mathematical Model

As we know that the result of braking torque from MRB is affected by shear stress between the MRB and the material in MRB. Bingham Model could predict the properties of MRF that expressed to Eq. (4) [25,27]

$$\tau = \tau_y(B) + \tau_\eta \tag{4}$$

where τ is shear stress, $\tau_y(B)$ is shear stress that depends on the magnetic field, and τ_η is shear stress that independent on the magnetic field. It is the combination of shear stress that on-state condition and off-state condition. Both of them can be expressed as follows [27]

$$\tau_y(B) = 52.962B^4 - 176.51B^3 + 158.78B^2 + 13.708B + 0.1442 \tag{5}$$

$$\tau_\eta = \eta \frac{r\dot{\theta}}{g} \tag{6}$$

where B is magnetic flux density, η is the viscosity of MRF, r is the radius of rotor, $\dot{\theta}$ is the angular velocity, and g is the gap of MRF. To find the braking torque in MRB, we can start from the basic torque that is shown on Eq. (7)

$$dT = \tau r dA \tag{7}$$

where r is the radius from the center of rotation across dA. Because MRB has a round shape, the coordinate must be changed into the polar coordinate. We can use a jacobian coordinate that changes into [30]

$$dT = \tau r^2 dr d\theta \tag{8}$$

From Eq. (8), there is two differentiation that can be derivate. The design of MRB have to spin 360°, so that it has limited from 0 until 2π that can refer to

$$T = 2\pi \int r^2 \tau \, dr \tag{9}$$

Refer Eq. (4) to Eq. (9) yields

$$T = 2\pi \int r^2 (\tau_y(B) + \tau_\eta) \, dr \tag{10}$$

Eq. (10) can be separated based on on-state and off-state conditions shown respectively on Eq. (11) and Eq. (12)

$$T_\tau = 2\pi \int r^2 \tau_y(B)\ dr \tag{11}$$

$$T_\eta = 2\pi \int r^2 \tau_\eta\ dr = 2\pi \int r^2 \eta \frac{r\dot{\theta}}{g}\ dr \tag{12}$$

In this case, the braking torque involves four components: those are radial T-leg (Tr_1), radial T-flange (Tr_2), annular inner (Ta_1), and outer annular (Ta_2). Figure 3 shows the schematic for four components.

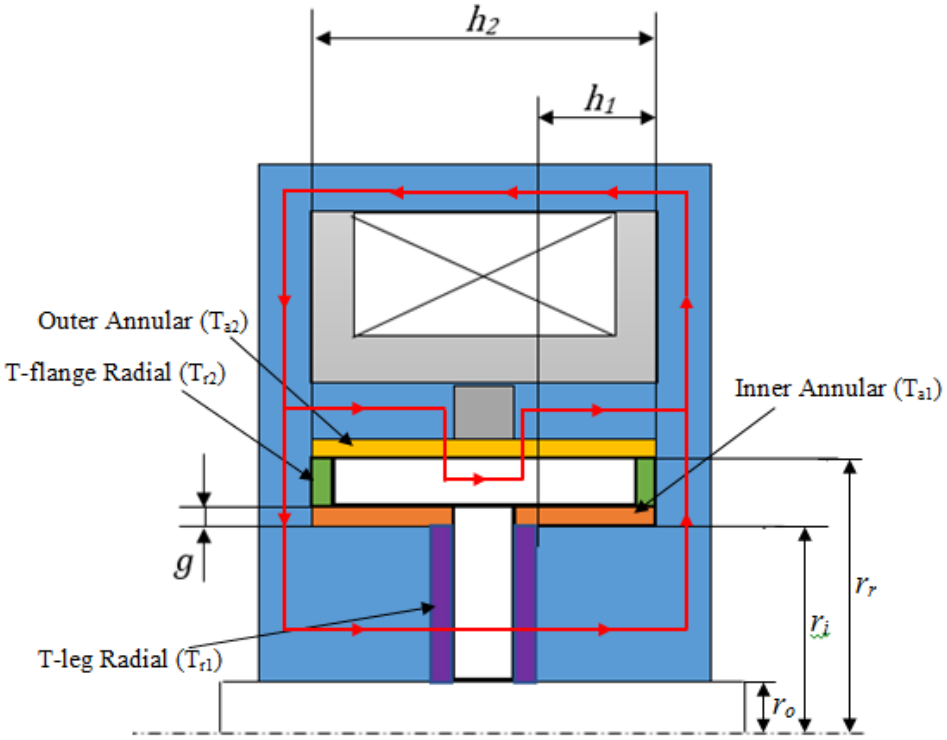

Fig. 3. Design of simulation FEMM

In Figure 3, radial T-leg has the limit r_o until r_i, that so torque for this component can be described off-state and on-state respectively to Eq. (13) and Eq. (14)

$$T_{\eta\ radial\ 1} = 2\pi \int_0^{r_i} r^3 \eta \frac{\dot{\theta}}{g} dr = \frac{\pi\eta\dot{\theta}(r_i^4 - r_o^4)}{2g} \tag{13}$$

$$T_{\tau\ radial\ 1} = 2\pi \int_0^{r_i} r^2 \tau_y\ dr = \frac{2}{3}\pi\tau_y(r_i^3 - r_o^3) \tag{14}$$

For another component, the way Eq. (13) and Eq. (14) can be used to get a governing equation

$$T_{\tau\ radial\ 2} = \frac{2}{3}\pi\tau_\tau(B)(r_r^3 - r_i^3) \tag{15}$$

$$T_{\tau\ annular\ 1} = 2\pi\tau_y(B) r_i^2 h_1 \tag{16}$$

$$T_{\tau\ annular\ 2} = 2\pi\tau_y(B)r_r^2 h_2 \quad (17)$$

$$T_{\eta\ radial\ 2} = \frac{\pi\eta\dot{\theta}(r_r^4 - r_i^4)}{2g} \quad (18)$$

$$T_{\eta\ annular\ 1} = \frac{2h_1\eta\dot{\theta}r_i^3}{g} \quad (19)$$

$$T_{\eta\ annular\ 2} = \frac{2h_2\eta\dot{\theta}r_r^3}{g} \quad (20)$$

where *h* is annular channel length. Table 4 shows the base MRB dimensions.

Table 4
Base MRB dimensions

No	Symbol	Description	Value (mm)
1	g	MRF gap	0.25
2	r_o	Shaft Radius	3.5
3	r_i	Inner radius	8.5
3	r_r	Outer radius	12.5
4	h_1	Annular channel length 1	8
5	h_2	Annular channel length 2	19

2.4 Experimental Setup

Figure 4 shows the configuration of experimental work. Shaft rotary torque transducer TCS-1000 KC 5kgf.cm ~ 1,000kgf.cm or torque sensor produced by CTAplus, Korea, was used. It used an inline method with two shafts to connect MRB and motor using jaw coupling that suitable for measuring continuous rotating torque. It also worked on low torque with input voltage 10 V. It consisted of a strain gage bridge that measures rotary torque.

A DC motor was used as a driving source powered by a power supply. The encoder was needed to ensure a constant angular velocity of 50 RPM. Encoder Cytron B 106, Malaysia, was used because of high accuracy, small size, and has minimum input voltage. MRB had been applied at 0-1 A current with an increment of 0.1 A. the current supplied would make the friction between the rotor and MRF inside MRB that could generate more braking torque.

The torque sensor generates analog signals that may be harmful to the monitor device if measure directly. It needed signal conditioning to make rough data from the torque sensor to be safe and legible. Data Acquisition National Instrument USB 6211, USA, was used for signals conditioning and receiving the signals from the torque sensor and encoder. It had an input voltage that suitable to TCS-1000 KC. Signals from data acquisition would be processed and displayed on the computer with LabVIEW software.

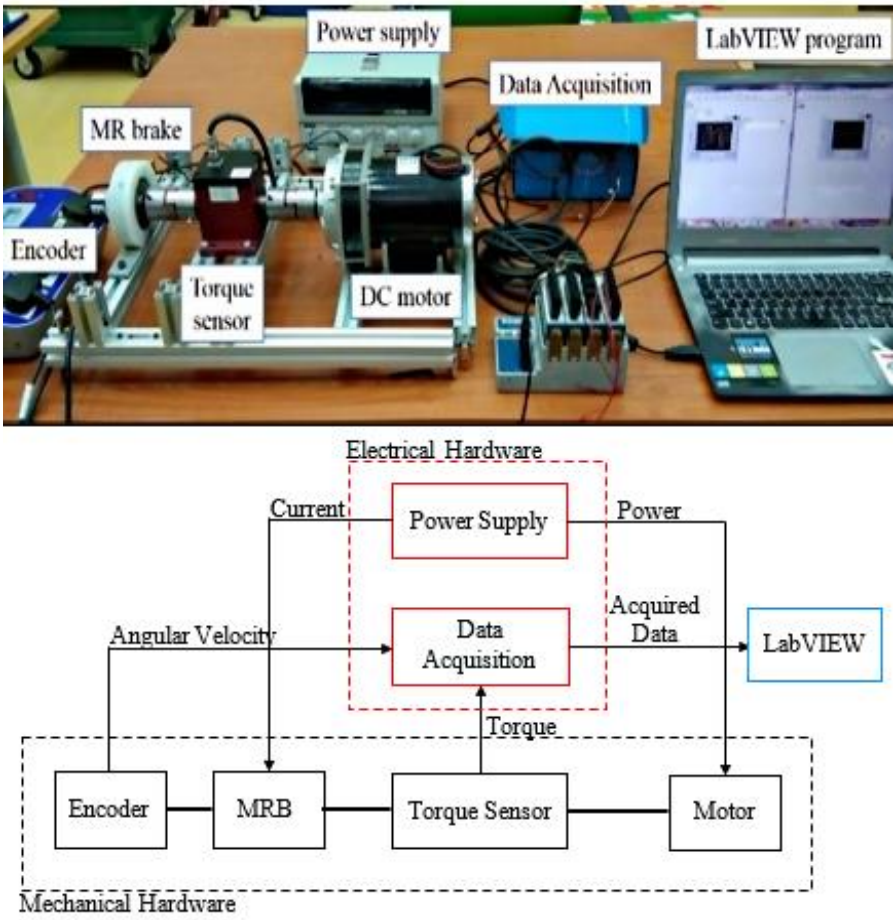

Fig. 4. Configuration of MRB test rig

3. Results

3.1 Simulation Result

Figure 5 shows the model of magnetostatics simulation. Lines around MRB show the magnetic flux pathways that only passed on magnetic material. On the outer annular, there is a turning flux groove due to the configuration of magnetic and non-magnetic materials on the stator. The red line in the MRF gap is a reference line for making plot magnetic flux density along the length. The different colors show different magnetic flux density. The darker color shows the more excellent value of magnetic flux density.

The electric current affects the magnetic flux density. The more significant current used, the greater the magnetic flux density generated. However, the increase is not the same as the initial growth because the direction of the magnetic flux is increasingly squeezed on the wall. Figure 6 shows the distribution of magnetic flux density along the MRF gap with different variations of electric current. The largest magnetic flux density is 0.45 T at the peak of the outer annular. It can be concluded that the outer annular gives higher contribution generated higher braking torque. The magnetic flux density obtained is used to calculate shear stress caused by the magnetic field.

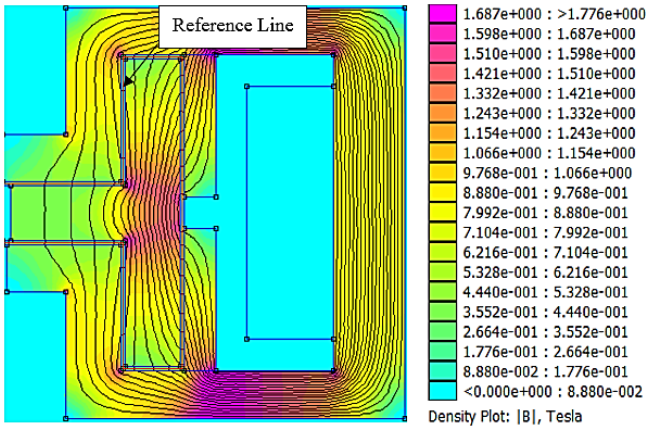

Fig. 5. Model of magnetostatics simulation

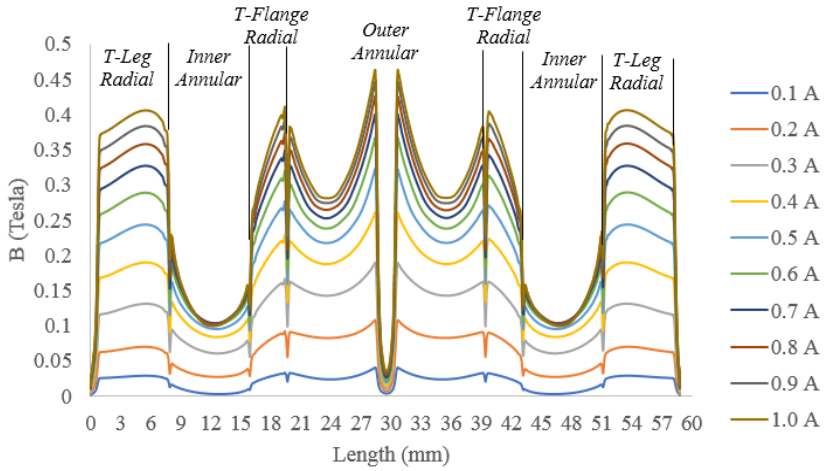

Fig. 6. Distribution of magnetic flux density along the MRF gap

3.2 Experimental Result

The experimental work was successfully carried out. TCS-1000 KC has recorded the braking torque from MRB. Figure 7 shows the result of braking torque along electric current based on both mathematical model and experimental work on constant angular speed 50 RPM and input current 0.1-1 A with interval 0.1 A each test.

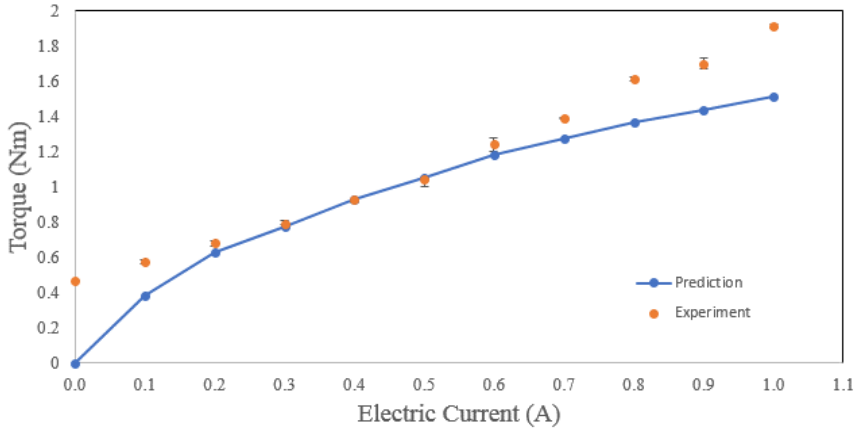

Fig. 7. Result of braking torque along with electric current

On both mathematical model and experimental work, it can be noted that the increase of current supplied, braking torque also increases. However, the increment braking torque is not as much as in the beginning. It was appropriate with the increment of magnetic flux density. There are some errors in both the mathematical model and experimental work. There is small braking torque in the mathematical model that almost 0 Nm on the 0 A while in experimental work was 0.46 Nm. The maximum braking torque on the mathematical model is 1.51 Nm, and the experiment is 1.91 Nm. Table 5 shows details of braking torque error each current supplied.

Table 5
Braking torque errors between the mathematical model and experimental work

Current (A)	Mathematical model (Nm)	Experiment work (Nm)	Error (%)
0	0.000254565	0.469291276	99.94576
0.1	0.379187284	0.571073314	33.60094
0.2	0.629073046	0.684576616	8.107722
0.3	0.778380779	0.79274927	1.812489
0.4	0.929225234	0.926541621	-0.28964
0.5	1.054340085	1.047166247	-0.68507
0.6	1.179279703	1.246856944	5.419807
0.7	1.274330349	1.393616604	8.559474
0.8	1.363926183	1.613290009	15.45685
0.9	1.435660659	1.698145582	15.45715
1	1.514851983	1.911518152	20.75137

3.3 Discussion

The new design of MRB T-shaped that had a more compact structure than Hidayatullah was made [25]. It would give smaller and lighter MRB. A smaller MRF gap would save more MRF, so that reduces costs. The usage of a smaller wire diameter could add more turn that would generate more magnetic flux density.

On the FEMM result, the maximum magnetic flux density was 0.45 T. It is better than Ubaidillah [12] but worse than Senkal [11], Hidayatullah [25], and Nguyen [26]. It would be caused by better reluctance that made flux magnetic smaller. The permeability for each material would also affect reluctance [19]. It could be seen at the difference of magnetic flux density results from other research that use different materials [25,27].

In Figure 7, the independent variable was electric current. It holds the main control to generate braking torque. The derivation of Bingham Model at Eq. (14), Eq. (18), Eq. (19), and Eq. (20) also present velocities as the independent variable that can be changed easily. But the changes in braking torque are not significant. From the LORD Corp. datasheet [28], a big shear rate affected by angular velocity is needed to generate big shear stress that could. It had done on another paper [19]. It was also done by Attia [15] with angular velocity 100, 200, and 300 RPM.

There are differences in braking torque between modelling and experiment. At 1 A, there is an error of 20%. There is also an error of 0.4 Nm at the off-state condition. The installation of the seal on MRB affect the friction that made shear stress higher. The error has been made by other MRB [20,22]. Low-friction seals could be used for the next research. Adding friction equation on the seal also used to get the same results with experimental work.

The braking torque generated was less than 2 Nm. It is small if we compare it with another T-shaped MRB like Hidayatullah [25] generated 2.1 Nm and Avraam [17] 22.5 Nm. The smaller size was the problem generated less torque from another MRB design that utilizes less MRF gap than a bigger one.

Braking torque also affected on the configuration. With a similar size, Ubaidillah [27] only get braking torque 0.26 Nm while it could generate higher although magnetic flux density was smaller. It had radial lengths of 1.6-2 times and annular lengths of 2-5 times. The configuration also affects the ability of magnetic flux to reach the MRF gap. Nguyen [26] and Avraam [17] need double wire turn to get almost all MRF gaps while it only uses a single wire turn using the serpentine magnetic flux principle. It would save more power while using MRB.

4. Conclusions

Braking torque of serpentine magnetic flux T-shaped MRB had carried out. The result from the FEMM simulation shown that the magnetic flux could reach in almost all the MRF gap with the maximum magnetic flux density of 0.45 T in the outer annular component. The braking torque has also been explained based on simulation and experimental work. The maximum braking torque for the mathematical model was 1.51 Nm, while the experimental work was 1.91 Nm at the electric current of 1 A. Overall, the errors between simulation and experimental work were about 10%. It could be shown that the mathematical model could be used for future research. Low-friction seals and friction equation could be used in the future to get a better result.

Acknowledgement

Authors thank for the collaboration between Universitas Sebelas Maret and Universitas Widyagama Malang. Universitas Sebelas Maret provides in-kind support and partial funding for prototype development. Universitas Widyagama offers full funding for the research through DRPM research Grant PDUPT UWG 2020.

References

[1] Ubaidillah, Sutrisno, Joko, Agus Purwanto, and Saiful Amri Mazlan. "Recent progress on magnetorheological solids: materials, fabrication, testing, and applications." *Advanced engineering materials* 17, no. 5 (2015): 563-597. https://doi.org/10.1002/adem.201400258

[2] Choi, H. J., S. A. Mazlan, and Fitrian Imaduddin. "Fabrication and viscoelastic characteristics of waste tire rubber based magnetorheological elastomer." *Smart Materials and Structures* 25, no. 11 (2016): 115026. https://doi.org/10.1088/0964-1726/25/11/115026

[3] Ahmad Khairi, M. H., and S. A. Mazlan. "Ubaidillah; Ku Ahmad, KZ; Choi, SB; Abdul Aziz, SA; Yunus, NA The field-dependent complex modulus of magnetorheological elastomers consisting of sucrose acetate isobutyrate ester." *J. Intell. Mater. Syst. Struct* 28 (2017): 1993-2004. https://doi.org/10.1177/1045389X16682844

[4] Spaggiari, Andrea, Davide Castagnetti, Nicola Golinelli, Eugenio Dragoni, and Giovanni Scirè Mammano. "Smart materials: Properties, design and mechatronic applications." *Proceedings of the Institution of Mechanical Engineers, Part L: Journal of Materials: Design and Applications* 233, no. 4 (2019): 734-762. https://doi.org/10.1177/1464420716673671

[5] Mangal, S. K., and Vivek Sharma. "On state rheological characterization of MRF 122EG fluid using various techniques." *Materials Today: Proceedings* 4, no. 2 (2017): 637-644. https://doi.org/10.1016/j.matpr.2017.01.067

[6] Dai, Jun, Hui Chang, Rui Zhao, Jue Huang, Kaiquan Li, and Saipeng Xie. "Investigation of the relationship among the microstructure, rheological properties of MR grease and the speed reduction performance of a rotary micro-brake." *Mechanical Systems and Signal Processing* 116 (2019): 741-750. https://doi.org/10.1016/j.ymssp.2018.07.004

[7] Sohn, Jung Woo, Juncheol Jeon, Quoc Hung Nguyen, and Seung-Bok Choi. "Optimal design of disc-type magneto-rheological brake for mid-sized motorcycle: experimental evaluation." *Smart Materials and Structures* 24, no. 8 (2015): 085009. https://doi.org/10.1088/0964-1726/24/8/085009

[8] Park, Bong Jun, Fei Fei Fang, and Hyoung Jin Choi. "Magnetorheology: materials and application." *Soft Matter* 6, no. 21 (2010): 5246-5253.

https://doi.org/10.1039/c0sm00014k
[9] Pokaad, Alif Zulfakar Bin, Khisbullah Hudha, and Mohd Zakaria Bin Mohamad Nasir. "Simulation and experimental studies on the behaviour of a magnetorheological damper under impact loading." *International Journal of Structural Engineering* 2, no. 2 (2011): 164-187.
[10] Imaduddin, Fitrian, Saiful Amri Mazlan, and Hairi Zamzuri. "A design and modelling review of rotary magnetorheological damper." *Materials & Design* 51 (2013): 575-591. https://doi.org/10.1016/j.matdes.2013.04.042
[11] Senkal, Doruk, and Hakan Gurocak. "Compact MR-brake with serpentine flux path for haptics applications." In *World Haptics 2009-Third Joint EuroHaptics Conference and Symposium on Haptic Interfaces for Virtual Environment and Teleoperator Systems*, pp. 91-96. IEEE, 2009. https://doi.org/10.1109/WHC.2009.4810807
[12] Imaduddin, Fitrian, Muhammad Nizam, and Saiful A. Mazlan. "Response of a magnetorheological brake under inertial loads." *International Journal on Electrical Engineering and Informatics* 7, no. 2 (2015): 308.
[13] Farjoud, Alireza, Nader Vahdati, and Yap Fook Fah. "Mathematical model of drum-type MR brakes using Herschel-Bulkley shear model." *Journal of Intelligent Material Systems and Structures* 19, no. 5 (2008): 565-572. https://doi.org/10.1177/1045389X07077851
[14] Yu, Jianqiang, Xiaomin Dong, and Wen Wang. "Prototype and test of a novel rotary magnetorheological damper based on helical flow." *Smart Materials and Structures* 25, no. 2 (2016): 025006. https://doi.org/10.1088/0964-1726/25/2/025006
[15] Attia, E. M., N. M. Elsodany, H. A. El-Gamal, and M. A. Elgohary. "Theoretical and experimental study of magneto-rheological fluid disc brake." *Alexandria Engineering Journal* 56, no. 2 (2017): 189-200. https://doi.org/10.1016/j.aej.2016.11.017
[16] Hudha, Khisbullah, and Hishamuddin Jamaluddin. "Simulation and experimental evaluation on a skyhook policy-based fuzzy logic control for semi-active suspension system." *International Journal of Structural Engineering* 2, no. 3 (2011): 243-272. https://doi.org/10.1504/IJSTRUCTE.2011.040783
[17] Avraam, More, Mihaita Horodinca, Pierre Letier, and André Preumont. "Portable smart wrist rehabilitation device driven by rotational mr-fluid brake actuator for telemedecine applications." In *2008 IEEE/RSJ International Conference on Intelligent Robots and Systems*, pp. 1441-1446. IEEE, 2008. https://doi.org/10.1109/IROS.2008.4650887
[18] Gudmundsson, K. H., F. Jonsdottir, and F. Thorsteinsson. "A geometrical optimization of a magneto-rheological rotary brake in a prosthetic knee." *Smart materials and Structures* 19, no. 3 (2010): 035023. https://doi.org/10.1088/0964-1726/19/3/035023
[19] Karakoc, Kerem, Edward J. Park, and Afzal Suleman. "Design considerations for an automotive magnetorheological brake." *Mechatronics* 18, no. 8 (2008): 434-447. https://doi.org/10.1016/j.mechatronics.2008.02.003
[20] Sarkar, C., and H. Hirani. "Design of a squeeze film magnetorheological brake considering compression enhanced shear yield stress of magnetorheological fluid." In *Journal of Physics: Conference Series*, vol. 412, no. 1, p. 012045. 2013. https://doi.org/10.1088/1742-6596/412/1/012045
[21] Imaduddin, Fitrian, Saiful Amri Mazlan, Hairi Zamzuri, and Abdul Yasser Abd Fatah. "Testing and parametric modeling of magnetorheological valve with meandering flow path." *Nonlinear Dynamics* 85, no. 1 (2016): 287-302. https://doi.org/10.1007/s11071-016-2684-6
[22] Kikuchi, Takehito, and Keigo Kobayashi. "Design and development of cylindrical MR fluid brake with multi-coil structure." *Journal of System Design and Dynamics* 5, no. 7 (2011): 1471-1484. https://doi.org/10.1299/jsdd.5.1471
[23] Nguyen, Q. H., and S. B. Choi. "Optimal design of an automotive magnetorheological brake considering geometric dimensions and zero-field friction heat." *Smart Materials and Structures* 19, no. 11 (2010): 115024. https://doi.org/10.1088/0964-1726/19/11/115024
[24] Poznić, A., A. Zelić, and L. Szabó. "Magnetorheological fluid brake–basic performances testing with magnetic field efficiency improvement proposal." *Hungarian Journal of Industry and Chemistry* (2012): 107-111.
[25] Hidayatullah, Faishal Harish, Endra Dwi Purnomo Ubaidillah, Dominicus Danardono Dwi Prija Tjahjana, and Ilham Bagus Wiranto. "Design and simulation of a combined serpentine T-shape magnetorheological brake." *Indonesian Journal of Electrical Engineering and Computer Science* 13, no. 3 (2019): 1221-1227. https://doi.org/10.11591/ijeecs.v13.i3.pp1221-1227
[26] Hung, Nguyen Q., and Choi S. Bok. "Optimal design of a T-shaped drum-type brake for motorcycle utilizing magnetorheological fluid." *Mechanics based design of structures and machines* 40, no. 2 (2012): 153-162.

https://doi.org/10.1080/15397734.2011.616479
[27] Ubaidillah, Wibowo, D. Adiputra, D. D. D. P. Tjahjana, M. A. A. Rahman, and S. A. Mazlan. "Performance prediction of serpentine type compact magnetorheological brake prototype." *AIPC* 1788, no. 1 (2017): 030032. https://doi.org/10.1063/1.4968285
[28] C. Load. "MRF-132DG Magneto-Rheological Fluid." *Lord Prod. Sel. Guid. lord Magnetorheol. fluids* 54, no. 2 (2011): 11.
[29] Meeker, David. "Finite element method magnetics, version 4.2." *User's Manual, University of Virginia, USA* (2009).
[30] Falcão da Luz, Luís. "Design of a magnetorheological brake system." (2004).